

## CHANDRA OBSERVATION OF THE RELATIVISTIC BINARY J1906+0746

O. KARGALTSEV<sup>1</sup> AND G. G. PAVLOV<sup>2</sup>

*Draft version July 18, 2021*

### ABSTRACT

PSR J1906+0746 is a young radio pulsar ( $\tau = 112$  kyr,  $P = 144$  ms) in a tight binary ( $P_{\text{orb}} = 3.98$  hr) with a compact high-mass companion ( $M_{\text{comp}} \simeq 1.36M_{\odot}$ ), at the distance of about 5 kpc. We observed this unique relativistic binary with the *Chandra* ACIS detector for 31.6 ks. Surprisingly, not a single photon was detected within the  $3''$  radius from the J1906+0746 radio position. For a plausible range of hydrogen column densities,  $n_{\text{H}} = (0.5\text{--}1) \times 10^{22}$  cm<sup>-2</sup>, the nondetection corresponds to the 90% upper limit of  $(3\text{--}5) \times 10^{30}$  erg s<sup>-1</sup> on the unabsorbed 0.5–8 keV luminosity for the power-law model with  $\Gamma = 1.0\text{--}2.0$ , and  $\sim 10^{32}$  erg s<sup>-1</sup> on the bolometric luminosity of the thermal emission from the NS surface. The inferred limits are the lowest known for pulsars with spin-down properties similar to those of PSR J1906+0746. We have also tentatively detected a puzzling extended structure which looks like a tilted ring with a radius of  $1.6'$  centered on the pulsar. The measured 0.5–8 keV flux of the feature,  $\approx 3.1 \times 10^{-14}$  erg cm<sup>-2</sup> s<sup>-1</sup>, implies an unabsorbed luminosity of  $1.2 \times 10^{32}$  erg s<sup>-1</sup> ( $4.5 \times 10^{-4}$  of the pulsar's  $\dot{E}$ ) for  $n_{\text{H}} = 0.7 \times 10^{22}$  cm<sup>-2</sup>. Although all conventional interpretations of the ring appear to be problematic, the pulsar-wind nebula with an unusually underluminous pulsar remains the most viable interpretation.

*Subject headings:* pulsars: individual (PSR J1906+0746) — stars: neutron — X-rays: ISM

### 1. INTRODUCTION

*Chandra* and *XMM-Newton* observations of isolated young and middle-aged pulsars reveal X-ray emission from the neutrons star (NS) surfaces and magnetospheres as well as extended emission from pulsar wind nebulae (PWNe; see Kargaltsev & Pavlov 2008 for a recent review; KP08 hereafter). The analysis of the X-ray properties of the pulsars and PWNe observed with *Chandra* shows a large scatter in their X-ray efficiencies,  $\eta_{\text{X}} = L_{\text{X}}/\dot{E}$  (e.g.,  $10^{-5} \lesssim \eta_{\text{X}} \lesssim 10^{-1}$  for the combined pulsar and PWN emission; KP08; Li et al. 2008). Among the most underluminous are several young pulsars,  $\tau \sim 30\text{--}100$  kyr, some of which have not been detected (e.g., PSR J1913+1011, which has the lowest known X-ray efficiency,  $\eta < 8 \times 10^{-6} d_5^2$ ; KP08). Although some of the very low efficiencies could be due to an underestimated distance, the growing number of underluminous pulsars (Newman et al., in preparation) and the very different efficiencies of pulsars with well known distances suggest that the inaccurate distances can be only part of the story.

PSR J1906+0746 (hereafter PSR J1906) was discovered by Lorimer et al. (2006) in the ALFA Arecibo Pulsar Survey (Cordes et al. 2006). PSR J1906 is a young, 144 ms pulsar in a highly relativistic orbit ( $P_{\text{orb}} = 3.98$  hr) with eccentricity  $e = 0.085$  and gravitational wave coalescence time of 300 Myr. The companion mass of  $(1.36 \pm 0.02)M_{\odot}$  (Kasian et al. 2007), the substantial eccentricity of the binary orbit, the small spin-down age ( $\tau = P/2\dot{P} = 112$  kyrs), the significant spin-down energy loss rate ( $\dot{E} = 2.7 \times 10^{35}$  erg s<sup>-1</sup>), and the relatively high magnetic field ( $B \approx 1.7 \times 10^{12}$  G) suggest that the pulsar could be a young, second-born NS in the double NS binary (DNSB) J1906+0746 (hereafter J1906). In this case we would expect the companion to be a millisecond pulsar (similar to PSR J0737–3039A in the double pulsar binary J0737–3039),

recycled during an earlier phase of accretion. However, despite deep radio searches, the second pulsar in J1906 has not been detected, perhaps because of the unfavorable orientation of its radio beam (Lorimer et al. 2006). Alternatively, J1906 could be similar to the NS binary J1141–6545, in which the companion is a massive,  $0.99 \pm 0.02M_{\odot}$ , white dwarf (WD) on an eccentric orbit around the 1.45 Myr old pulsar<sup>3</sup> (Kaspi et al. 2000; Bailes et al. 2003). A main sequence companion is ruled out by the binary evolution scenarios (see e.g., Stairs 2004, and references therein) unless the binary companions did not evolve together (i.e., the binary was formed recently through a gravitational capture).

The recent discoveries of X-ray emission from the tight pulsar binaries J0737–3039 (McLaughlin et al. 2004; Campana et al. 2004; Pellizzoni et al. 2004, 2008), B1534+12 (Kargaltsev et al. 2006) and B1957+20 (Stappers et al. 2003) have drawn substantial interest to the high-energy emission mechanisms in such systems, particularly because one can infer the properties of pulsar winds and binary companions via observations of X-ray emission from intrabinary shocks. Although relatively distant, J1906 appears to be a good candidate for detecting X-ray emission from yet another tight NS binary because PSR J1906 is young and energetic (e.g., the  $L_{\text{X}}\text{--}\dot{E}$  relation from Possenti et al. 2002 predicts the nonthermal X-ray luminosity of  $\simeq 10^{32}$  erg s<sup>-1</sup> in 2–10 keV). This prompted us to carry out an exploratory *Chandra* observation, results of which we describe below.

### 2. OBSERVATIONS AND DATA ANALYSIS

We observed J1906 with the Advanced CCD Imaging Spectrometer (ACIS) aboard *Chandra* on 2007 August 10 (start time 54,322.0374098 MJD). The useful scientific exposure time was 31,610 s. The observation was carried out in Very Faint mode, and the pulsar was imaged  $45.8''$  off-axis on the I3 chip of the ACIS-I array (the other activated chips were I0,

<sup>1</sup> Dept. of Astronomy, University of Florida, Bryant Space Science Center, Gainesville, FL 32611; oyk100@astro.ufl.edu

<sup>2</sup> The Pennsylvania State University, 525 Davey Lab, University Park, PA 16802, USA; pavlov@astro.psu.edu

<sup>3</sup> A somewhat older,  $\tau \approx 30$  Myrs, pulsar B2303+46 is also known to be in a binary with a factor of 60 wider eccentric orbit and  $(1.3 \pm 0.1)M_{\odot}$  WD companion (van Kerkwijk & Kulkarni 1999).

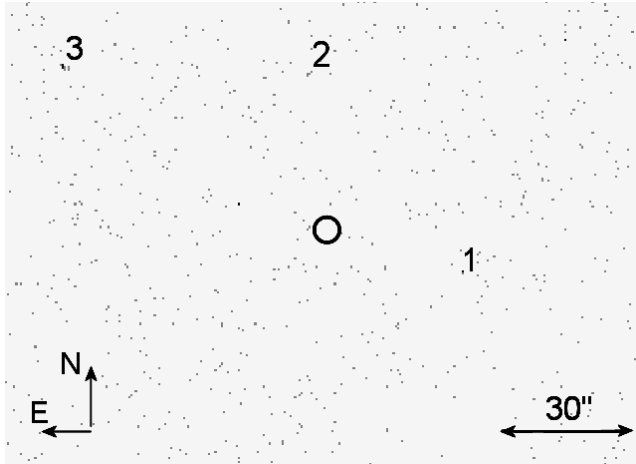


FIG. 1.— ACIS image of the J1906 vicinity (pixel size  $0.492''$ ) in the 0.5–8 keV band. The circle ( $R = 3''$ ) is centered on the radio position of PSR J1906 (Lorimer et al. 2006). There are no X-ray counts within this circle. Notice that the quoted uncertainty of the radio position is much smaller than the circle shown (see text). The three nearby sources are numbered according to Table 1.

TABLE 1  
X-RAY SOURCES NEAR THE RADIO POSITION OF PSR J1906

# <sup>a</sup>	$\Delta^b$	R. A.	Decl.	$N_{0.5-2}^c$	$N_{2-8}^d$
1	$33.2''$	$19^{\text{h}}06^{\text{m}}46^{\text{s}}.529$	$07^{\circ}46'18''.47$	4	0
2	$36.7''$	$19^{\text{h}}06^{\text{m}}48^{\text{s}}.954$	$07^{\circ}47'04''.84$	4	0
3	$72.8''$	$19^{\text{h}}06^{\text{m}}52^{\text{s}}.846$	$07^{\circ}47'06''.47$	7	2

<sup>a</sup>Source number in Figure 1.

<sup>b</sup>Angular separation from the radio pulsar position.

<sup>c</sup>Number of counts in 0.5–2 keV band.

<sup>d</sup>Number of counts in 2–8 keV band.

I1, I2 and S3). The detector was operated in Full Frame mode, which provides a time resolution of 3.24 s. The data were reduced using the *Chandra* Interactive Analysis of Observations (CIAO) software (ver. 4.0; CALDB ver. 3.4.0). To maximize the signal-to-noise ratio, we choose the energy range of 0.5–8 keV for the imaging and spectral analysis.

### 2.1. X-ray data

We found no X-ray source near the pulsar’s radio position R.A.= $19^{\text{h}}06^{\text{m}}48^{\text{s}}.673(6)$ , Decl.= $07^{\circ}46'28''.6(3)$  reported by Lorimer et al. (2006) from radio timing. Figure 1 shows that there are no photons in the 0.5–8 keV band within the  $3''$  radius circle around the radio position. This radius is a factor of 8 larger than the  $0.37''$  uncertainty obtained by adding in quadratures the uncertainties of the radio-timing position ( $\sigma_r = 0.31''$ ) and the *Chandra* aspect solution ( $\sigma_a \approx 0.2''$ ; e.g., Pavlov et al. 2009, and references therein). Therefore, we conclude that J1906 is not detected in the *Chandra* ACIS image. The three nearest X-ray sources (with  $\geq 4$  counts in the  $r = 1.5''$  aperture) are offset by  $33''$ – $73''$  from the radio pulsar position (see Figure 1 and Table 1).

We have used circular annuli centered on the pulsar radio position to measure the local background count rate out to  $r = 30''$  from the pulsar. We find the background to be rather uniform (the surface brightnesses measured from the individual annuli are consistent with a constant surface brightness within the uncertainties). The mean background surface brightness is  $0.035 \pm 0.003$  counts arcsec $^{-2}$ . Thus, within the  $r = 3''$  extraction aperture one would expect to detect about

one count from the background. For a Poissonian distribution, the nondetection with zero counts translates into the upper limit  $N < -\ln(1 - \text{CL})$  counts at the confidence level CL, which gives the 90% count rate upper limit of  $7.3 \times 10^{-5}$  counts  $\text{s}^{-1}$ .

To constrain the absorption in the direction toward J1906, we fit the spectrum of the brightest X-ray source in the field (marked X in Fig. 2) located at the edge of the ACIS-I field-of-view ( $\approx 11'$  west of J1906 at R.A.=  $19^{\text{h}}06^{\text{m}}06^{\text{s}}.6$  and Decl.=  $07^{\circ}42'58''$ ). The spectrum (total 176 counts in the 0.5–8 keV band, of which 11% are from the background) fits well ( $\chi^2_\nu = 0.74$  for  $\nu = 14$ ) an absorbed power-law (PL) model with photon index  $\Gamma = 1.3 \pm 0.2$  and hydrogen column density  $n_{\text{H},22} \equiv n_{\text{H}}/10^{22} \text{ cm}^{-2} = 1.1 \pm 0.3$ . On the other hand, the PSR J1906’s dispersion measure  $\text{DM} = 218 \text{ pc cm}^{-3}$  gives  $n_{\text{H},22} = 0.65$ , assuming 10% ISM ionization. Finally, the total Galactic HI column in the direction toward J1906 (galactic coordinates:  $l = 41.60^\circ$ ,  $b = 0.15^\circ$ ) is  $n_{\text{HI},22} = 1.5$ – $1.9$ , according to Dickey & Lockman (1990), while Kalberla et al. (2005) give a slightly lower value,  $n_{\text{HI},22} = 1.4$ – $1.6$ . The distance to the edge of the Galaxy in this direction is  $\sim 15$  kpc, while the distance to J1906, based on the pulsar’s dispersion measure, is about 5 kpc (4.5 kpc and 5.4 kpc for the galactic electron density distributions by Taylor & Cordes 1993 and Cordes & Lazio 2002, respectively; we will scale all distance-dependent quantities to  $d = 5$  kpc below). Thus, a plausible range for the absorbing column toward J1906 is  $n_{\text{H},22} \approx 0.5$ – $1.0$ .

To calculate the upper limits on the X-rays fluxes from PSR J1906 and its putative compact PWN, we consider two plausible spectral models: (1) a nonthermal PL spectrum from the pulsar magnetosphere and/or from a compact unresolved PWN, and (2) a thermal spectrum emitted from the NS surface. We then calculate the upper limits on the 0.5–8 keV unabsorbed flux as a function of photon index for the PL model (Fig. 3) and on the bolometric luminosity as a function of the NS surface temperature for the blackbody (BB) model (Fig. 4), using *Chandra* PIMMS<sup>4</sup> for  $n_{\text{H},22} = 0.5, 0.7$ , and  $1.0$ . The implications of these results are discussed in §§ 3.1 and 3.2.

We have also searched the ACIS image for extended X-ray emission on larger angular scales. The images in Figures 2 and 5 show a hint of a puzzling elliptical structure (resembling a tilted ring with a radius of  $\approx 1.6'$ ) approximately centered on the J1906 position. To assess the statistical significance of the feature, we extracted the surface brightness profile from a set of 12 elliptical annuli (see Fig. 5). A  $\chi^2$  fit with a constant background (fitted to the first 7 bins in Fig. 5, bottom) shows that the brightness enhancement is significant at a  $3.9\sigma$  level. We have also extracted the ring spectrum from the elliptical annulus that includes the entire diffuse ring. The total number of extracted counts is 467, with the background<sup>5</sup> contributing 81%. The number of net source counts is  $90 \pm 24$  in the same energy range. After binning the spectrum heavily ( $\approx 90$  counts per spectral bin) and subtracting the background, we fitted an absorbed PL model (see Fig. 6) to the spectrum of the ring. For the fixed  $n_{\text{H},22} = 0.7$ , the spectrum fits the absorbed PL model with the photon index  $\Gamma = 1.6 \pm 0.7$  and the unabsorbed 0.5–8 keV flux of  $(4.0 \pm 0.8) \times 10^{-14} \text{ erg s}^{-1} \text{ cm}^{-2}$  ( $\chi^2_\nu = 0.98$  for  $\nu = 3$ ).

<sup>4</sup> See <http://cxc.harvard.edu/toolkit/pimms.jsp>

<sup>5</sup> The background was extracted from a factor of four larger area, including a region inside the ring as well as regions outside the ring. The latter regions were selected on the same chip and the same CCD nodes as those covered by the ring, with background point sources excluded.

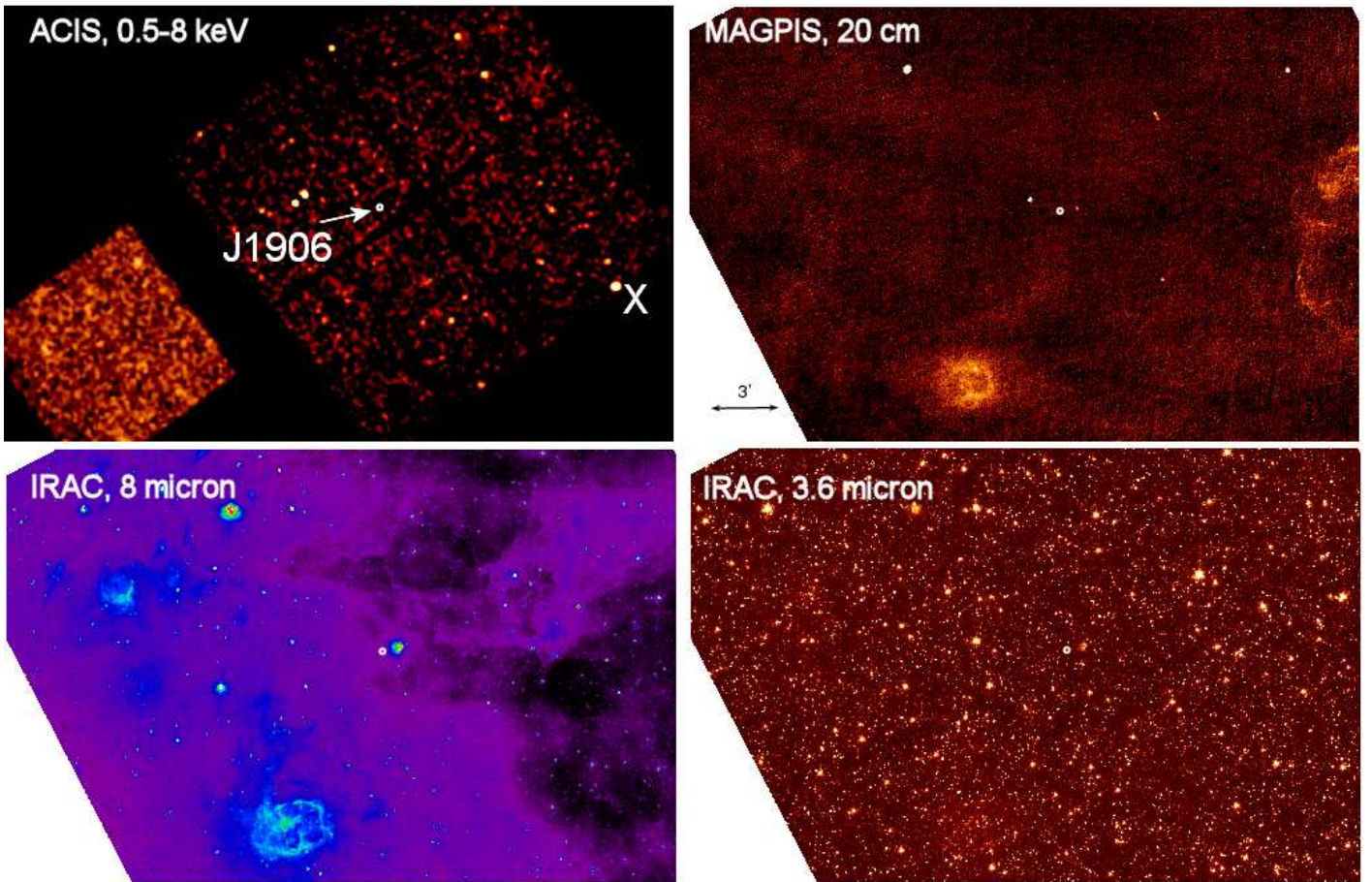


FIG. 2.—  $18' \times 29'$  images of the J1906 field at different wavelengths. The radio position of J1906 is shown by the small circle. The ACIS image is binned to  $2''$  pixels and smoothed with an  $r = 6''$  gaussian kernel.

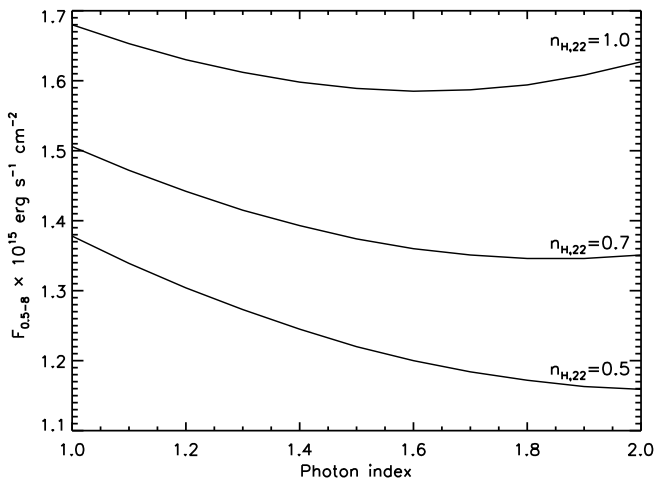


FIG. 3.— Upper limits on the unabsorbed flux of J1906 in the 0.5–8 keV band as functions of photon index for the PL spectral model, computed for three plausible  $n_{\text{H}}$  values.

## 2.2. Multiwavelength Data

To examine the J1906 field at other wavelengths, we have searched IR and radio survey data. Figures 2 and 7 show *Spitzer* IRAC images<sup>6</sup> at 8 and  $3.6 \mu\text{m}$  and radio images from

<sup>6</sup> The IRAC images are from the GLIMPSE (Galactic Legacy Infrared Mid-Plane Survey Extraordinaire) data (Benjamin et al. 2003; see also <http://irsa.ipac.caltech.edu/data/SPITZER/GLIMPSE/>)

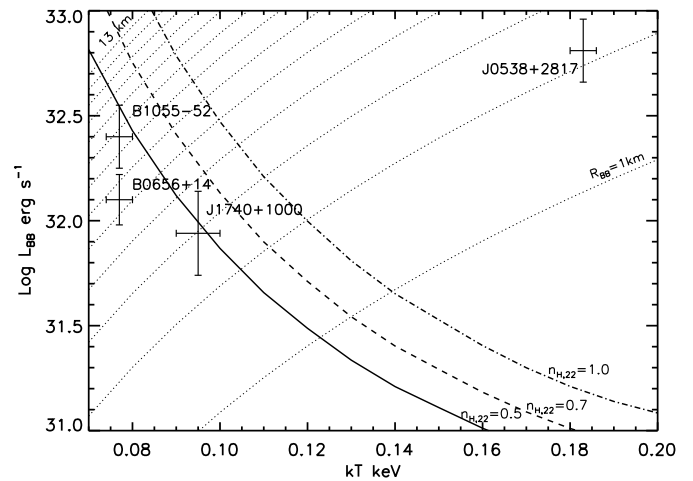


FIG. 4.— Upper limits on the bolometric luminosity of thermal emission from the surface of PSR J1906, assuming a single-temperature absorbed BB model. The limits are plotted for  $n_{\text{H},22} = 0.5, 0.7, \text{ and } 1$ , within a plausible range of BB temperatures as measured in pulsars with ages similar to that of J1906. The bolometric luminosities of these pulsars (based on single-component BB fits; see text for details) are plotted for comparison. The dotted lines are loci of constant BB radii (increasing from lower right to upper left in 1 km increments).

VLA MAGPIS<sup>7</sup>. PSR J1906 is detected in the 20 cm MAGPIS image, with the flux of  $0.66 \pm 0.27$  mJy (consistent within

<sup>7</sup> See White et al. (2005); also <http://third.ucllnl.org/gps/>.

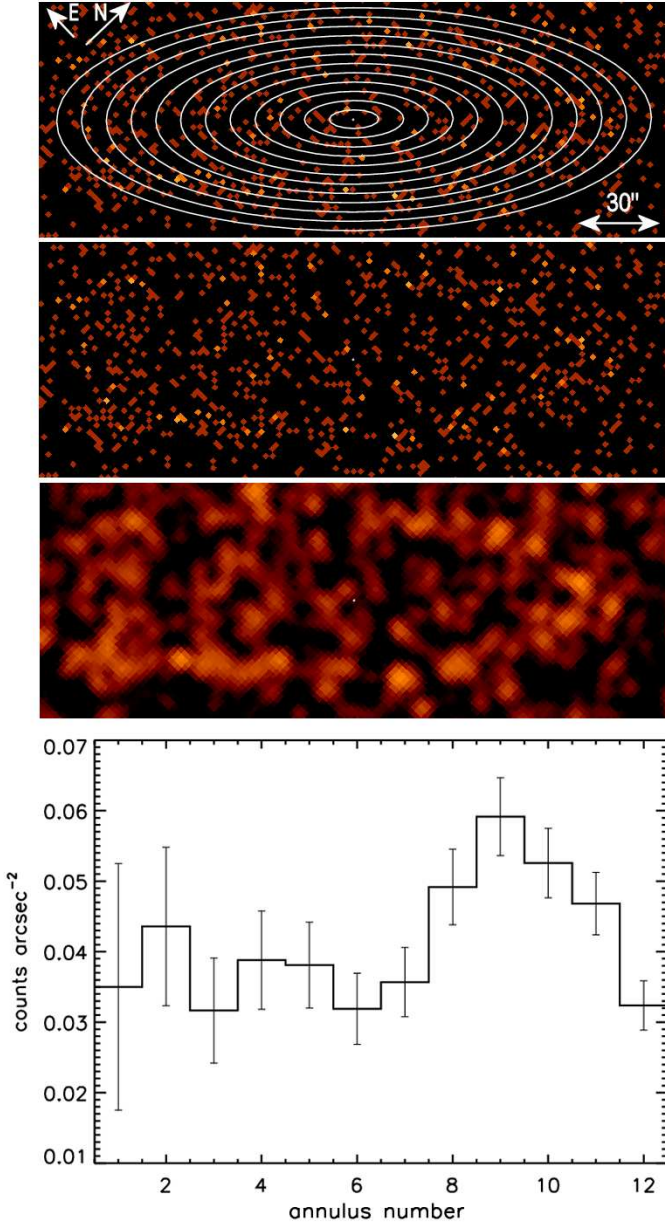


FIG. 5.— Three top panels show  $4' \times 1.5'$  ACIS images of the J1906 vicinity (in 0.5–8 keV, pixel size  $1.97''$ ; the same part of the sky is shown in all the images). The top image shows the elliptical annuli (centered on the PSR J1906 radio position) used to characterize the ring-like structure discussed in §3.1. The bottom image is smoothed with the  $6''$  gaussian. The bottom panel shows the average surface brightness distribution as a function of the annulus number (counted outwards from the center).

the uncertainties with the  $0.55 \pm 0.15$  mJy flux measured by Lorimer et al. 2006 in the 1.3–1.5 GHz band from the timing observations). The measured  $1.0'' \pm 0.5''$  offset between the MAGPIC position and the radio-timing position of PSR J1906 is consistent with both sources being the same object.

The IR images also reveal a bright ( $\approx 0.03, 1.7, 4.3, 48.3$  and  $105$  Jy at  $4.5, 12, 25, 60$  and  $100 \mu\text{m}$ , respectively<sup>8</sup>) diffuse source IRAS 19043+0741,  $\sim 46''$  west of J1906. The source has a radio counterpart, GPSR5 41.594+0.160, with the flux of 4.4 mJy at 5 GHz (Becker et al. 1994). The bow-like shape of the diffuse source seen in the  $8 \mu\text{m}$  image and

<sup>8</sup> The IR fluxes are taken from the GLIMPSE I Spring 2007 Catalog and the IRAS Point Source Catalog (ver. 2.1), available at the NASA IPAC Infrared Science Archive, <http://irsa.ipac.caltech.edu/applications/BabyGator/>.

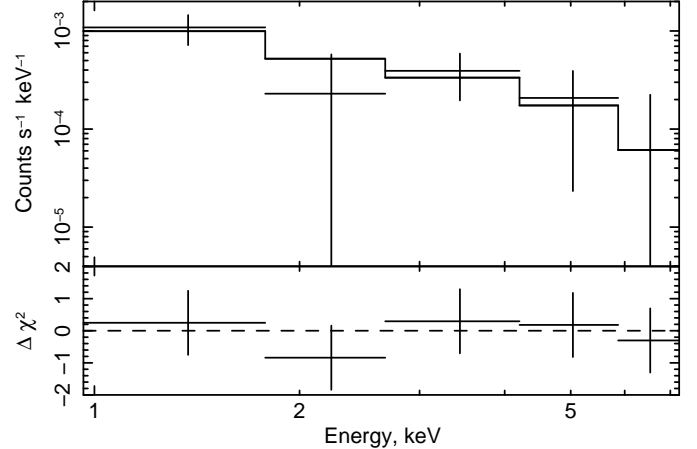


FIG. 6.— Spectrum of the ring (see §2.1) fitted with the absorbed PL model ( $\Gamma = 1.6 \pm 0.7$  and fixed  $n_{\text{H},22} = 0.7$ ; see §2.1).

a hint of two tails seen in the VLA image create an impression that the source is moving westward. The source is listed as a star-forming region in two catalogs (Codella et al. 1995; Avedisova 2002). No X-ray counterpart of this source has been identified in the ACIS data. There is no reason to believe that J1906 was born in IRAS 19043+0741 since J1906 would have to be traveling at a speed of  $\sim 10,000$  km  $\text{s}^{-1}$  to reach its current position, assuming the same 5 kpc distance to the two sources and a 10 Myr travel time (considered to be an upper limit for an age of a star-forming region; e.g., Hartmann 2001). Thus, we conclude that IRAS 19043+0741 is an unrelated object accidentally projected near J0906.

Most of the X-ray point sources seen in the images do not have counterparts at other wavelengths (e.g., the sources in Table 1 have no 2MASS counterparts), with a possible exception for the source #3 (in Fig. 1 and Table 1) located  $\approx 72.8''$  northeast of the pulsar (i.e., outside the X-ray ring), which apparently has a relatively bright (26 mJy at 1.4 GHz) radio counterpart NVSS 190654+074715 but no IR counterpart. We did not find any traces of the putative tilted ring (§2.1) at any frequencies other than X-rays. A large number of very faint background sources (e.g., stars) might, in principle, mimic the diffuse emission at least in some parts of the putative ring. However, the  $3.6 \mu\text{m}$  image does not reveal an enhanced stellar density along the ring (see Fig. 7) and hence does not support this interpretation.

### 3. DISCUSSION

To date, X-ray emission has been detected from two DNSBs (J0737–3039 and B1534+12; McLaughlin et al. 2004 and Kargaltsev et al. 2006). In both cases no extended X-ray PWN has been seen. However, the pulsars in these DNSBs are much older and less energetic than PSR J1906. The only tight binary with a pulsar (although not a DNSB) whose PWN has been resolved in X-rays (Stappers et al. 2003) is the famous “Black Widow” binary, in which the wind of the energetic PSR B1957+20 ablates the surface of the low-mass dwarf companion. Since PSR J1906 is even more energetic than PSR B1957+20, one could expect it to be easily detectable in X-rays. Yet, we have not detected a single photon from J1906 in the 31.6 ks *Chandra* ACIS observation. We, however, discovered a puzzling diffuse emission shaped as an elliptical ring centered on the pulsar. Below we discuss a possible origin of the ring, the upper limits on the J1906 X-ray luminosity, and the constraints on the physical properties of this unique system.

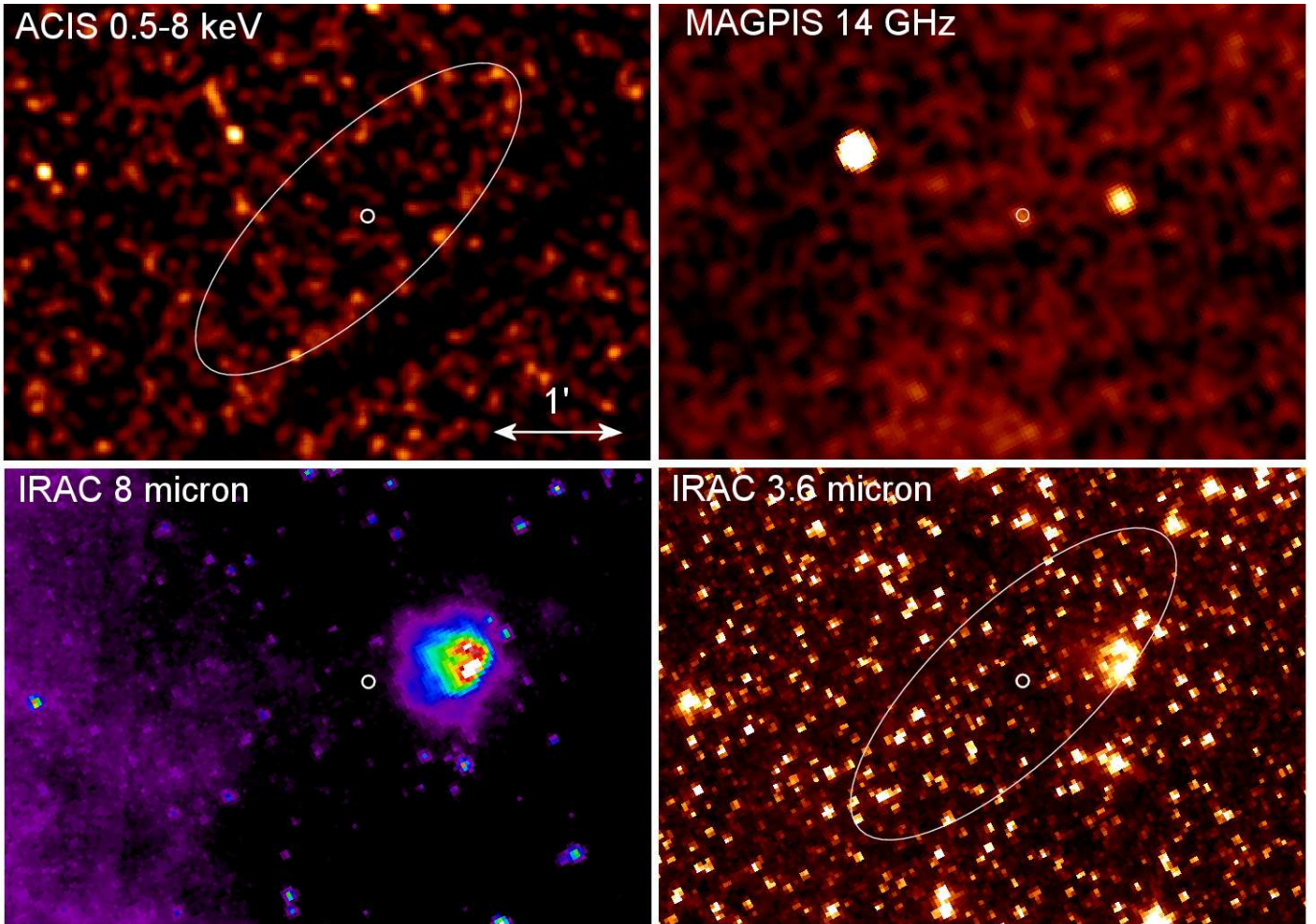


FIG. 7.—  $3.6' \times 5.0'$  images of the J1906 field at different wavelengths (the same region of sky is shown in all the panels). The radio position from Lorimer et al. (2006) corresponds to the center of the circle with  $7''$  radius. The ellipse shows the region of enhanced X-ray emission shaped as an elliptical ring approximately centered on J1906. The same ellipse is shown on the 3.6-micron image. The ACIS image is binned to  $0.98''$  pixels and smoothed with an  $r = 5''$  gaussian kernel.

PSR J1906 is sufficiently young and energetic to power a detectable X-ray PWN. One can also expect to see thermal X-ray emission from the hot surface of the 100-kyr-old NS and possibly non-thermal emission from the pulsar's magnetosphere. In addition, the presence of a NS (or heavy WD) companion might perturb the PSR J1906 wind and give rise to an additional emission component from an intrabinary shock. However, in J1906 the latter component should be much fainter compared to the other emission components mentioned above. Indeed, if the J1906 companion is a WD, then the solid angle subtended by the WD,  $\Delta\Omega \simeq (R_{\text{WD}}/2a)^2 = 1.3 \times 10^{-6} (R_{\text{WD}}/2 \times 10^8 \text{ cm})^2 \text{ sr}$ , is so small that the WD cannot intercept a significant fraction of the pulsar's wind, even if the wind is strongly anisotropic. The fraction of the intercepted wind could be larger if the companion is a NS because in this case the effective cross section would be determined by the standoff distance, at which the magnetic pressure of the companion's magnetosphere is equal to the pressure of the pulsar's wind (e.g., Kargaltsev et al. 2006). It should be noted, however, that the companion NS is likely significantly older than PSR J1906 because it takes at least  $10^6$ – $10^7$  years to spin up this first-formed NS and expel the outer layers of its companion (progenitor of PSR J1906) through the common envelope phase, thereby shrinking the binary orbit to its current size. In addition, the first-born NS would only retain a weak magnetic field,  $\lesssim 10^{10}$  G, after a long period of

accretion. Thus, if the J1906's companion NS has properties similar to those of PSR J0737–3039A, then the size of the compressed companion magnetosphere,  $\sim 7 \times 10^8$  cm (see eq. [1] in Arons et al. 2005), is comparable to a typical WD radius, i.e., only a small fraction of the J1906's wind would be intercepted. Thus, one would expect the observed X-ray properties of the J1906 PWN to be such as what they would be if the PWN were powered by a solitary pulsar.

Finally, one could expect to see X-ray emission from the companion if it is indeed a NS. However, according to the evolutionary scenarios (see above) the companion NS is expected to be much older, with a colder surface and lower  $\dot{E}$ . Hence, its X-ray emission is expected to be significantly fainter than that of PSR J1906.

### 3.1. Limits on the nonthermal X-ray emission from the pulsar and unresolved compact PWN.

The upper limit on the combined unabsorbed flux from the compact, unresolved PWN and the pulsar's magnetosphere, estimated as described in §2.1, is  $(1.1 - 1.7) \times 10^{-15} \text{ erg cm}^{-2}$  at 90% confidence, in the 0.5–8 keV band (see Fig. 3). This flux corresponds to the luminosity  $L_X < (3.3 - 5.1) \times 10^{30} d_5^2 \text{ erg s}^{-1}$  and efficiency  $\eta_X < (1.2 - 1.9) \times 10^{-5} d_5^2$ . Compared to other pulsar + PWN systems, the inferred upper limits are unusually low, albeit not the most extreme. This is seen from Figure 8, in which we plotted the 0.5–8 keV pulsar + PWN luminosities for about 40 detected systems, and a

few upper limits, versus pulsar’s spin-down power  $\dot{E}$  (see also KP08). In particular, the pulsar + PWN luminosities and efficiencies for the objects with similar  $\dot{E}$  values are a factor of a few higher than the J1906’s upper limits (see Table 2). Yet, there is a younger, more energetic pulsar, J1913+1011, from which no counts were detected in a 20 ks *Chandra* ACIS-S3 observation, and for which the upper limit on the pulsar + PWN efficiency is even lower than for J1906 (see Fig. 8). The nondetection of pulsars could be attributed to an unfavorable orientation of the X-ray beams, but it is more difficult to explain the nondetection of PWNe, whose emission should be more isotropic (and which are, on average, a factor of  $\sim 4$  more luminous in X-rays than their pulsars; Kargaltsev et al. 2007).

Thus, although the X-ray efficiency of the J1906 PWN is within the range of efficiencies measured for the entire sample of pulsar + PWN sources, J1906 is among the most underluminous ones. We should stress that the observed *four orders of magnitude* scatter in  $\eta_X$  cannot be attributed just to poorly measured distances, and therefore better understanding of pulsar wind physics is needed to explain the very different X-ray pulsar + PWN efficiencies.

### 3.2. Interpretation of the ring: An unusual PWN?

The nature of the tentatively detected ring-like structure (see §2.1) is puzzling. One might assume that the ring is a limb-brightened shell of the remnant of the supernova in which PSR J1906 was born. However, the size of the shell is too small for a SNR of a 100 kyr age. For instance, in the Sedov regime, the SNR radius can be estimated as  $\simeq 21'(E_{51}/n)^{1/5}(t/100 \text{ kyrs})^{2/5}d_5^{-1}$  (where  $E = 10^{51}E_{51} \text{ erg s}^{-1}$  is the SN energy release, and  $n$  is the ambient matter density in units of  $\text{cm}^{-3}$ ), much larger than the  $1.6'$  semimajor axis of the observed ellipse, at reasonable values of the parameters. To explain the ellipsoidal shape of the shell, an unusual density distribution in the ambient medium would be required. Moreover, it is hard to expect such a narrow, distinct shell for so old SNR. Finally, the spectrum of the elliptical ring ( $\Gamma = 1.6 \pm 0.7$ , detected up to 7 keV, albeit with a scant statistic) is too hard for an SNR shell (its slope is typical for a PWN spectrum, however; KP08). Therefore, we do not consider the SNR shell interpretation to be plausible.

Alternatively, one could attempt to interpret the ring as synchrotron emission produced immediately downstream of the termination shock in the pulsar wind. Although such structures have been seen in many PWNe (e.g., the rings around the Crab and J1930+1852 pulsars), the X-ray emission from the pulsar (or its unresolved vicinity) is usually more luminous than that of the ring (see Fig. 2 in KP08). The only apparent exception is the PWN in the IC 443 SNR (Gaensler et al. 2006; Weisskopf et al. 2007), where the alleged pulsar (pulsations are yet to be found) is a factor of 10 dimmer (in terms of the 0.5–8 keV flux) than the surrounding bright PWN emission associated with the termination shock (which, however, is not clearly resolved into a ring in this case). The nondetection of PSR J1906 implies that it is at least a factor of 20–40 dimmer than the ring. The reasons for such a low pulsar-to-PWN flux ratio could be a special orientation of the magnetic and rotation axes resulting in suppressed magnetospheric activity, or the presence of absorbing matter near the pulsar (Cordes & Shannon 2008). In addition to the problematic flux ratio, the observed size of the ring requires stretching the limits on other physical parameters. Since most of the PSR J1906’s wind es-

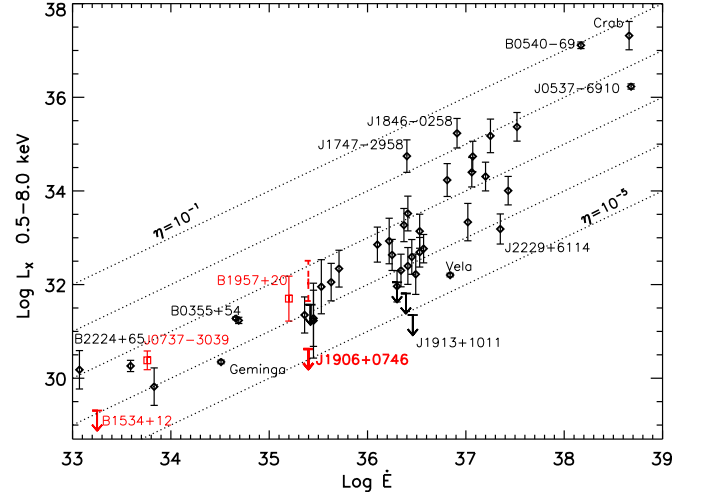


FIG. 8.— Summed nonthermal 0.5–8 keV luminosities of pulsar + PWN systems observed with *Chandra* versus pulsar’s spin-down power. The tight pulsar binaries discussed in the paper are shown in red. The dashed red errorbar corresponds to the luminosity of the elliptical ring which might be an extended PWN associated with J1906.

capas unperturbed by the interaction with the companion (see above), the termination shock in the pulsar wind would occur at  $R_{TS} \approx (\dot{E}f_w/4\pi cP_{amb})^{1/2} = 0.085f_w^{1/2}P_{amb,-11}^{-1/2} \text{ pc}$  (it corresponds to the angular distance of  $3.5''f_w^{1/2}P_{amb,-11}^{-1/2}d_5^{-1}$ ), where  $P_{amb} \equiv 10^{-11}P_{amb,-11} \text{ dyne cm}^{-2}$  is the ambient pressure, and the factor  $f_w$  takes into account possible anisotropy of the pulsar wind (e.g., Kargaltsev et al. 2006). This distance is much smaller than the  $1.6'$  radius of the putative tilted ring, unless the pulsar wind is extremely well collimated in the equatorial plane and/or the ambient pressure is very low (e.g.,  $f_w \sim 100$ ,  $P_{amb,-11} \sim 0.1$ ). These requirements can, however, be relaxed if the pulsar is substantially closer than 5 kpc (measuring the pulsar’s parallax is needed to establish the distance reliably). On the other hand, the unabsorbed luminosity of the ring,  $L_X = (1.2 \pm 0.3) \times 10^{32}d_5^2 \text{ erg s}^{-1}$  for the plausible  $n_{H,22} = 0.7$ , gives the X-ray efficiency  $\eta_X = 4.5 \times 10^{-4}d_5^2$ , typical for a PWN (see the dashed errorbar in Fig. 8).

Another conceivable interpretation of the observed structure might be a “light echo” caused by reflection from dust following a hypothetical flare (e.g., due to an accretion episode) that could occur in the binary in the recent past (e.g., a few years ago). We know nothing about the putative flare, nor about the dust distribution around the system. However, the elliptical shape of the structure would require a very special dust distribution. In this scenario, which currently seems rather unlikely, a subsequent observation might show an increased size of the structure.

Finally, there still remains a possibility that the ring-like structure might be caused by fluctuations in the detector background (which could be enhanced on one side because of the proximity to the chip edge<sup>9</sup>) and sky background (e.g., due to a number of faint, unresolved point sources, such as field stars, accidentally projected along the ellipse). A deeper *Chandra* observation, with the target placed farther from the chip gaps, can ascertain the reality of the enigmatic ring.

<sup>9</sup> However, we do not see an enhanced surface brightness in the regions adjacent to the boundaries of the other I-array chips.

### 3.3. Limits on thermal emission from the NS surface

The surface of a 100-kyr-old NS is expected to be hot enough to emit soft X-rays (Yakovlev & Pethick 2004, and references therein). The surface temperature is likely non-uniform, with polar regions being hotter than the rest of the NS surface (see, e.g., Pavlov et al. 2002; De Luca et al. 2005). The observation of J1906 allows us to put an upper limit on the bolometric luminosity,  $L_{\text{BB}} = 4\pi R^2 \sigma_{\text{SB}} T^4$ , of PSR J1906 and compare it with the luminosities of other pulsars of similar ages. Figure 4 shows the upper limits in the  $T$ - $L_{\text{BB}}$  plane, computed in a plausible range of temperatures for three  $n_{\text{H}}$  values, assuming a BB spectrum. The same figure shows the BB temperatures and bolometric luminosities for four other pulsars with similar spin-down ages<sup>10</sup>. We see from Figure 4 that the upper limit curves  $L_{\text{BB}}(T)$  for PSR J1906 ( $\tau = 112$  kyr) pass just slightly above the points corresponding to PSR J1740+1000 ( $\tau = 115$  kyr), B0656+14 ( $\tau = 110$  kyr), and B1055-52 ( $\tau = 537$  kyr). On the contrary, the point corresponding to PSR J0538+2817 ( $\tau = 617$  kyrs) lie substantially above the upper limit curves because of the high temperature (and small BB radius) of this pulsar. However, based on the measurements of the proper motion and parallax of PSR J0538+2817, which resides in the S147 SNR, its true age, 20–60 kyr, is much smaller than the spin-down age<sup>11</sup>, which may explain the high temperature (Ng et al. 2007). From the upper limits in Figure 4 we can conclude that PSR J1906 is unlikely to be significantly younger than its spin-down age, and the BB luminosity of PSR J1906 may be similar to those of the other three pulsars [ $L_{\text{BB}} \approx (1-3) \times 10^{32}$  erg s<sup>-1</sup>].

We should note that the single-component BB model, used above for the sake of comparison, provides only a crude approximation to the spectra of the thermally-emitting pulsars. For instance, the high-quality *XMM-Newton* spectrum of PSR J1740+1000, which is almost an exact twin of J1906 in terms of the spin-down properties, is much better described by a three-component model, with two BB components ( $kT \approx 70$  and 140 eV, and  $R \approx 5.8$  and 0.6 km, respectively) and a PL component with  $\Gamma = 1.2 \pm 0.3$  (Misanovic et al., in preparation). However, the bolometric luminosity of the low-temperature component,  $\simeq 1 \times 10^{32}$  erg s<sup>-1</sup>, is close to that inferred from the simplified BB description of the PSR J1740+1000's X-ray spectrum, thus supporting the simplified

<sup>10</sup> The parameters of the BB fits are from our own analysis, except for J0538+2817 (Zavlin & Pavlov 2004).

<sup>11</sup> The apparent discrepancy between the spin-down and kinematic ages can be eliminated if we assume that the pulsar was born with a period close

analysis described above.

## 4. SUMMARY

In the 31.6 ks *Chandra* ACIS observation we have not detected a single photon from the J1906 binary within the 3'' radius from its radio position. The nondetection of PSR J1906 and its compact PWN could be explained by several factors. The thermal X-ray emission from the surface of the middle-aged PSR J1906 is likely too strongly absorbed by the ISM to detect it in a short observation, but the upper limit on the bolometric BB luminosity only slightly exceeds the bolometric luminosities observed in pulsars of similar ages. The non-detection of the pulsar's magnetospheric emission might be explained by an unfavorable orientation of the pulsar beam. The lack of X-ray emission from an intrabinary shock can be explained by a small size of the intrabinary interaction region that intercepts only a tiny fraction of the PSR J1906 wind. However, the non-detection of a compact PWN around the J1906 binary is surprising; perhaps it could be ascribed to unusual properties of the ambient medium or of the pulsar itself.

We found tentative evidence of a puzzling elliptical ring centered on J1906, with a  $3.9\sigma$  significance; however, the size of the structure is significantly larger than the stand-off distance to the termination shock produced by an isotropic pulsar wind in a typical ISM. The PWN interpretation of the ring is not ruled out, but it requires a high degree of the pulsar wind collimation and a low density of the surrounding ISM, or a distance significantly smaller than estimated from the pulsar's dispersion measure. Deeper, high-resolution observations at X-ray and radio frequencies should help to clarify the nature of the observed diffuse structure and to unambiguously detect the elusive pulsar wind from this unique pulsar.

Support for this work was provided by the National Aeronautics and Space Administration through Chandra Award Number G07-8061X issued by the Chandra X-ray Observatory Center, which is operated by the Smithsonian Astrophysical Observatory for and on behalf of the National Aeronautics Space Administration under contract NAS8-03060. The work was also partially supported by NASA grant NNX09AC84G.

to its modern value (Ng et al. 2007).

## REFERENCES

- Avedisova, V. S. 2002, *Astronomy Reports*, 46, 193  
Arons, J., Backer, D. C., Spitkovsky, A., & Kaspi, V. M. 2005, in *Binary Radio Pulsars*, eds. F. A. Rasio & I. H. Stairs, ASP Conf. Ser., 328, 95  
Bailes, M., Ord, S. M., Knight, H. S., & Hotan, A. W. 2003, *ApJ*, 595, 49  
Becker, R. H., White, R. L., Helfand, D. J., & Zoonematkermani, S. 1994, *ApJS*, 91, 347  
Benjamin, R. A., et al. 2003, *PASP*, 115, 953  
Campana, S., Possenti, A., & Burgay, M. 2004, *ApJ*, 613, L53  
Chatterjee, S., Gaensler, B. M., Melatos, A., Brisken, W. F., & Stappers, B. W. 2007, *ApJ*, 670, 1301  
Codella, C., Palumbo, G. G. C., Pareschi, G., Scappini, F., Caselli, P., & Attolini, M. R. 1995, *MNRAS*, 276, 57  
Cordes, J. M., & Lazio, T. J. W. 2002, preprint (arXiv:astro-ph/0207156)  
Cordes, J. M., et al. 2006, *ApJ*, 637, 446  
Cordes, J. M., & Shannon, R. M. 2008, *ApJ*, 682, 1152  
De Luca, A., Caraveo, P. A., Mereghetti, S., Negroni, M., & Bignami, G. F. 2005, *ApJ*, 623, 1051  
Dickey, J. M., & Lockman, F. J. 1990, *ARA&A*, 28, 215  
Gaensler, B. M., Chatterjee, S., Slane, P. O., van der Swaluw, E., Camilo, F., & Hughes, J. P. 2006, 648, 1037  
Hartmann, L. 2001, *AJ*, 121, 1030  
Kalberla, P. M. W., et al. 2005, *A&A*, 440, 775  
Kargaltsev, O., Pavlov, G. G., & Garmire, G. P. 2006, *ApJ*, 646, 1139  
Kargaltsev, O., Pavlov, G. G., & Garmire, G. P. 2007, *ApJ*, 660, 1413  
Kargaltsev, O., & Pavlov, G. G. 2008, in *40 Years of Pulsars: Millisecond Pulsars, Magnetars, and More*, eds. C. Bassa, A. Cumming, V. M. Kaspi, & Z. Wang, AIP Conf. Proc., 983, 171 (KP08)  
Kargaltsev, O., Misanovic, Z., Pavlov, G. G., Wong, J. A., & Garmire, G. P. 2008, *ApJ*, 684, 542  
Kasian, L. 2008, in *40 Years of Pulsars: Millisecond Pulsars, Magnetars, and More*, eds. C. Bassa, A. Cumming, V. M. Kaspi, & Z. Wang, AIP Conf. Proc., 983, 485  
Kaspi, V. M., et al. 2000, *ApJ*, 543, 321  
Lorimer, D. R., et al. 2006, *ApJ*, 640, 428  
Li, X.-H., Lu, F.-J., & Li, Z. 2008, *ApJ*, 682, 1166  
McLaughlin, M. A., et al. 2004, *ApJ*, 605, L41

TABLE 2  
 PROPERTIES OF PULSARS WITH SPIN-DOWN PARAMETERS SIMILAR TO PSR J1906.

PSR	$P$ ms	$\log \tau$	$\log \dot{E}$	$d^a$ kpc	$n_{\text{H},22}^b$	Exp. <sup>c</sup> ks	$N_{\text{cts}}^d$ cts	$\log L_{\text{PSR}}^e$	$\log L_{\text{PWN}}^f$	$\log \eta_{\text{PSR}}^g$	$\log \eta_{\text{PWN}}^h$
J1906+0746	144	5.05	35.43	5	0.7	31.6	0	< 30.7	< 30.7[32.1]	< -4.7	< -4.7 [-3.3]
J1702-4128	182	4.74	35.53	5	1.1	10.4	8	$31.70 \pm 0.50$	$31.60 \pm 0.50$	-3.8	-3.9
J0729-1448	252	4.54	35.45	4	0.3	4.1	13	$31.30 \pm 0.30$	$31.20 \pm 0.50$	-4.1	-4.2
J1740+1000	154	5.06	35.36	1.4	0.1	5.1	130	$31.10 \pm 0.05$	$31.11 \pm 0.10$	-4.3	-4.3
J1841-0345	204	4.75	35.43	4	0.8	10.0	2	< 31.57	< 31.57	< -3.9	< -3.9

<sup>a</sup> Distance estimate based on the pulsar's dispersion measure.

<sup>b</sup> Hydrogen column density estimated from the pulsar's dispersion measure (assuming 10% ISM ionization).

<sup>c</sup> *Chandra* ACIS exposure time.

<sup>d</sup> Number of counts in the 0.5–8 keV band, calculated for an  $R = 3''$  circular aperture centered on the radio pulsar position.

<sup>e</sup> Logarithm of the pulsar luminosity (or 90% upper limit on the pulsar + compact PWN luminosity for undetected objects) in the 0.5–8 keV band. For J1740+1000, the quoted luminosity is for the PL component only; the total 0.5-8 keV luminosity,  $10^{32.05}$  erg s<sup>-1</sup>, is much higher because of the contribution of the thermal component.

<sup>f</sup> Logarithm of the PWN luminosity (or 90% upper limit on pulsar + compact PWN luminosity for undetected objects) in the 0.5–8 keV band. The luminosity for the J17400+1000 PWN does not include the very extended tail (Kargaltsev et al. 2008). For J1906, we also provide the luminosity of the putative ring in the brackets.

<sup>g</sup> Logarithm of the pulsar X-ray efficiency (or 90% upper limit).

<sup>h</sup> Logarithm of the PWN X-ray efficiency (or 90% upper limit).

Ng, C.-Y., Romani, R. W., Brisken, W. F., Chatterjee, S., & Kramer, M. 2007, *ApJ*, 654, 487  
 Pavlov, G. G., Zavlin, V. E., & Sanwal, D. 2002, in Proc. 270 WE-Heraeus Seminar on Neutron Stars, Pulsars, and Supernova Remnants, MPE Rep. 278, eds. W. Becker, H. Lesch, & J. Trümper (Garching bei München: Max-Planck-Institut für Extraterrestrische Physik), p.272  
 Pavlov, G. G., Kargaltsev, O., Wong, J. A., & Garmire, G. P. 2009, *ApJ*, 691, 458  
 Pellizzoni, A., De Luca, A., Mereghetti, S., Tiengo, A., Mattana, F., Caraveo, P., Tavani, M., & Bignami, G. F. 2004, *ApJ*, 612, L49  
 Pellizzoni, A., Tiengo, A., De Luca, A., Esposito, P., & Mereghetti, S. 2008, *ApJ*, 679, 664  
 Possenti, A., Cerutti, R., Colpi, M., & Mereghetti, S. 2002, *A&A*, 387, 993

Stairs, I. H. 2004, *Science*, 304, 547  
 Stappers, B. W., Gaensler, B. M., Kaspi, V. M., van der Klis, M., & Lewin, W. H. G. 2003, *Science*, 299, 1372  
 Taylor, J. H., & Cordes, J. M. 1993, *ApJ*, 411, 674  
 van Kerkwijk M. H. & Kulkarni S. R. 1999, *ApJ*, 516, L25  
 Weisskopf, M. C., Karovska, M., Pavlov, G. G., Zavlin, V. E., & Clarke, T. 2007, *Ap&SS*, 308, 151  
 White, R. L., Becker, R. H., & Helfand, D. J. 2005, *AJ*, 130, 586  
 Yakovlev, D. G., & Pethick, C. J. 2004, *ARA&A*, 42, 169  
 Zavlin, V. E. & Pavlov G. G. 2004, *Mem. Soc. Astron. Italiana*, 75, 458